Robot Controlled Data Acquisition System for Microwave Imaging

Nikola Petrovic[#1], Tommy Gunnarsson[#,*], Nadine Joachimowicz[*], Magnus Otterskog[#2]

[#]*School of Innovation, design and engineering, Mälardalen University,*

Box 883, 721 23 Västerås, Sweden

[1]nikola.petrovic@mdh.se

[2]magnus.otterskog@mdh.se

[*]*Laboratoire des Signaux et Systèmes, SUPÉLEC,*

3 rue Joliot-Curie, F-91192 Gif-sur-Yvette Cedex, France

***Abstract*— In this paper an experimental prototype of a robot controlled data acquisition system for microwave imaging is presented, where the transmitting and receiving antennas are immersed in a water-tank. The scattered field from the object under test is acquired by using the robot and scanning a single receiving antenna in cylindrical or half spherical coordinates, while the transmitting antenna is fixed at one position with possibilities to be manually moved to different positions. Careful design and construction of the system has given accurate measurements of incident and total field with a SNR of 45dB. A validation of the robot system is performed by comparing measured and computed data for a sunflower oil object.**

I. INTRODUCTION

The microwave imaging modality focusing a lot of interest nowadays as a non-destructive evaluation of materials and biological tissues, in terms of complex permittivity. Changes in the dielectric properties of tissues can be related to their physiological condition, opening for many biomedical applications. One application gaining a lot of interest recently is breast tumor detection as an alternative mammography modality [1], [2]. One potential is the high complex permittivity contrast between different in-vivo tissues (fat, glandular, malign tumor, etc.) in the microwave spectrum compared to e.g. the density contrast in the X-ray spectrum. However, the increased wavelength in the microwave spectrum increasing the difficulties while the high diffraction needing more sophisticated algorithms and puts high demands on the data acquisition system.

Various hardware and software setups for microwave imaging have been developed during the last three decades. The first successful experimental setup was made by Larsen and Jacobi in the early 80's, which resulted in images showing the internal structure of canine kidneys [3]. These results are historical and they established a proof of principle for microwave imaging of biological tissues.

Another hardware setup is the 2.45GHz planar microwave camera at Supélec in Paris developed by Bolomey *et al*. The planar microwave camera is composed with two horn antennas, one transmitter and one receiver. In the front of the receiving antenna a matrix of 32x32 =1024 sensors (dipole antennas) are used, a so called Modulated Scattering Technique (MST), to enable a quick data acquisition [4]-[6]. The next milestone was the 64 antenna circular 2.33GHz microwave imaging system developed by Jofre *et. al*. [7], [8]. The system, which presents a circular geometry, was proven to be a better choice for two-dimensional (2-D) imaging, than the planar geometry [7].

Later, Semenov *et al.* presented two circular microwave imaging systems in [9] and [10]. Similar to Semenov et *al.* Meaney *et al.* developed a circular microwave imaging system for reconstruction of 2-D electrical property distributions [1]. They were the first to develop a clinical prototype for active microwave imaging of the breast in the early 2000's [11]. The hardware has been designed to have each antenna operate in either transmit or receive mode. In this case they used 16 monopole antennas in a circular array configuration. Today one could say that this system is the state of the art regarding microwave imaging for breast cancer detection.

Still today many improvements of both algorithms and hardware are needed for microwave imaging to be considered as a reliable modality in clinical situations. Having studied the previous works, mentioned above, carefully and try include all the advantages of each system into a new feasible system, the challenge to design and develop a flexible hardware system for microwave imaging was conducted. Herein a new flexible robot controlled microwave imaging system is presented, able to measure the vertical polarized field along both cylindrical and half-spherical surfaces around the object. The objective is to achieve a flexible system able to be used in both hardware, (antennas and system geometry), and algorithmic investigations for future microwave imaging systems. One of the purposes with this system is to investigate the possibility of detecting early stage breast tumors with quantitative images. However, in this initial study a tube filled with sunflower oil is used to validate the system. We are currently designing more realistic breast phantoms for this purpose.

This paper is organized as follows. Section II presents the description of the robot controlled data acquisition system, including the experimental prototype system, the design and performance of the receiving and transmitting antennas, the positioning by the robot and the data acquisition ending with the explanation of the numerical tool used in the simulations. Section III explaining the experimental validation of the system. Finally, conclusions are given in section IV.

II. Robot Controlled Microwave Imaging System

A. System Overview

The main components of the system are an ABB robot (IRB140), a 2*m* diameter water-tank into which an object-fixture is immersed, two monopole antennas connected to a vector network analyzer (VNA) (Rohde&Schwarz ZV8), and a developed Matlab™ interface controlling the data acquisition. The entire setup is depicted in Fig. 1.

The receiving antenna is placed on the tip of the robot arm moving, along cylindrical or half-spherical surfaces, (other possible geometries could be programmed), around the object under examination. The radius and angular steps are adjustable for the different geometries before each examination. The object is positioned on a rotation axis in the center of the tank (center point of the system), controlled by a step motor. In this way multi-view examination is possible with an angular step as small as 1.8°. The transmitting antenna is fixed at one position through the examination, but can manually be moved to different positions. Through the examination the control interface receive wideband measurements from the VNA, at each position. First, the incident field (without the object) is measured before the total field (with the object present) is measured, in the form of S_{21}-parameters. The control interface storing data from both fields and the field scattered by the object can be computed by subtracting the incident field from the total field.

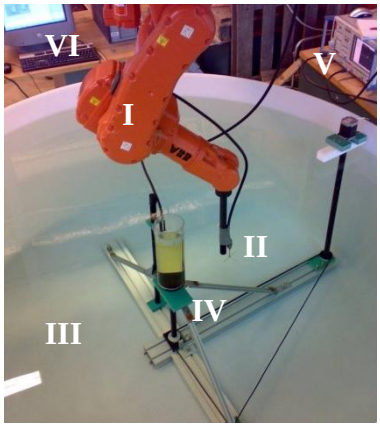

Fig. 1 Experimental setup of the robot controlled data acquisition system. The robot (I) with the receiving antenna (II), water-filled tank (III) with fixture (transmitting antenna, rotational board, object and step motor) (IV), VNA (V), and the PC (VI).

The advantages of the robot controlled microwave imaging system are: (1) the positioning of the receiving antenna is adjustable in a variety of geometries (2) high accuracy and stability in positioning the receiving antenna <0.1*mm*; (3) a flexible receiving antenna positioning enable investigations of different antenna array geometries without introducing coupling effects between multiple antenna elements in the system design stage; (4) a wideband system makes it possible to investigate suitable frequency band for the imaging application; and (5) a fast data acquisition time for broad band frequency measurements, which is 1s for each receiver position when the robot is using a very slow movement-mode.

B. Antenna Design and Performance

The electromagnetic fields are measured with a linearly polarized monopole antenna; an identical antenna is used for transmitting. A motivation for using the monopole antennas is that the monopole can be easily modeled as a line source in a 2-dimensional (2-D) imaging problem [1], [12]. The antennas are made of a semi rigid coaxial cable and the physical length of the inner conductor is 11*mm* designed to work in water with a complex permittivity of $\varepsilon^* = 83.2+j7.3$, estimated from the Stogryn's model [13]. The ground plane is designed as four rigid wires arranged in a cross, where each wire is perpendicular to the antenna depicted in Fig. 2. A design like that will not give a rotational symmetric radiation pattern in the horizontal plane, which implies to keep the orientation of the receiving antenna always in same direction in relation to the center point of the system. The return loss is below -14dB at 1 GHz for both antennas and they are broad banded in water from 950MHz – 1150MHz with return loss less than -10dB. The antennas are the critical points when choosing the usable frequency band of the system. However, other antennas for other frequencies or with a wider frequency band can be designed to gain from the wide band capability of the system.

Fig. 2 The receiving monopole antenna mounted on the robot arm

C. Geometrical Receiving Antenna Positioning

The usage of the robot to conduct data for microwave imaging gives an opportunity to evaluate different antenna configurations in a very rapid and straightforward way, while eliminating the interferences that an array of antennas might introduce. Due to the high precision, in the order smaller than tenths of a millimeter, the robot allows a good reproducibility of the measurement conditions.

The robot moves in the coordinate system with its origin at the center of the water-tank (the center of the measured object). To verify where the origin is, the object is calibrated in relation to the robots coordinate system. The examination object and the transmitting antenna can then be placed accordingly.

The receiving antenna can be moved along two types of patterns: cylindrical or half spherical. Several parameters can be chosen for each type of movement, such as radius, angular distance between points, the starting and ending frequencies, speed of the robot and number of points.

In the cylindrical movement, the following parameters are used as inputs: radius *r*, height of cylinder *hcyl*; angle between points, $step_\phi$, where ϕ is the angle relative to *x*-axis; $step_z$, the distance between points along the *z*-axis, to which the cylinder

is aligned; wideness of the measurement given in degrees. The target positions *p* will be given by:

$$p = \begin{cases} x = r\ \cos\phi \\ y = r\ \sin\phi \\ z = step_z\ \times n \end{cases}$$

The orientation of antenna's coordinate system can be described by a rotational matrix that describes the direction of the axes of the coordinate system in relation to a reference system. The antenna will always be parallel to the surface of the cylinder, and the orientation of the antenna is given by the following rotational matrices, depending on if *y* is positive or negative:

$$R_{y>0} = \begin{bmatrix} cos\ \phi & sin\ \phi & 0 \\ sin\ \phi & -cos\ \phi & 0 \\ 0 & 0 & -1 \end{bmatrix}$$

$$R_{y<0} = \begin{bmatrix} cos\ \phi & -sin\ \phi & 0 \\ -sin\ \phi & -cos\ \phi & 0 \\ 0 & 0 & -1 \end{bmatrix}$$

An example of a cylindrical pattern followed by the antenna will be similar to the one in Fig. 3. In this case, the measurement is 270° wide.

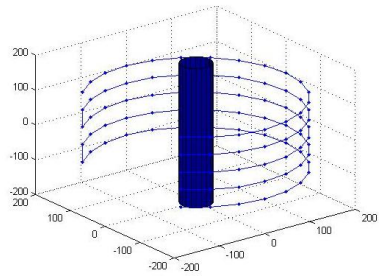

Fig. 3 An example of the path followed when in cylindrical pattern

Later on, also a spherical pattern could be used. In this case the input parameters for the spherical pattern are *r*, *step*θ, and *step*ϕ. Where *r* is the distance from the Tool Center Point (TCP) to the center of the measured object, *step*θ is the angular distance between points at the same height, and *step*ϕ is the angular distance between consecutive heights, relative to the *z*-axis, as shown in Fig. 4. The location of any measurement point *p* at the surface of the sphere is given by:

$$p = \begin{cases} x = r\ \cos\theta \sin\phi \\ y = r\ \sin\theta \sin\phi \\ z = r\ \cos\phi \end{cases}$$

Besides the position, the robot needs to know the orientation of the antenna, and with both, the *robot targets* are calculated.

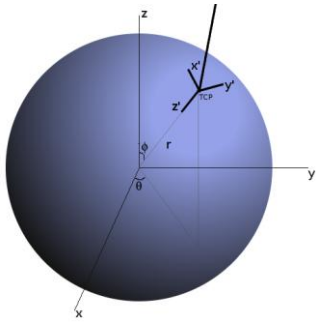

Fig. 4 Coordinate system in spherical measurements

The position and orientation values are calculated to each target and stored in an array, which is then used to move the robot. When the movement is started the first measurement target where the antenna goes is at the top of the sphere. It then follows a pattern similar to the one in Fig. 5. The change of direction is necessary because the robot has not the possibility to rotate more than 360°. When the last measurement target is reached, the robot returns to the default initial position, following exactly the same path. This is done to guarantee that the robot does not stop because one of its joints reached its limit.

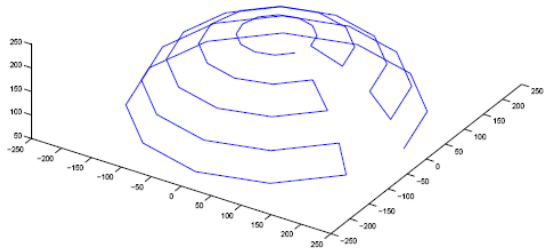

Fig. 5 Path followed when in spherical pattern

D. Data Acquisition

In order to coordinate the robot and the vector network analyzer (VNA), a Matlab program is used for communication and final data acquisition. The examination object positioned in the water-tank is illuminated by the electromagnetic field from the transmitting antenna and the receiving antenna collects the scattered field at different locations controlled by the robot system.

The VNA is measuring the fields in form of complex scattering parameters (*S*-parameters) between the transmitter and the receiver. The particular scattering parameter used is S_{21}, where the index 1 and 2 refer to the transmitter and receiver, respectively. This is repeated for each receiver position and stored in the Matlab interface as follows

$$\mathbf{E}^{\text{inc}}_{\text{meas}}(r) = \Phi \cdot S^{\text{inc}}_{21} \quad (1)$$

related to the incident field $\mathbf{E}^{\text{inc}}_{\text{meas}}(r)$ without an object in the imaging domain, and

$$\mathbf{E}^{\text{tot}}_{\text{meas}}(r) = \Phi \cdot S^{\text{tot}}_{21} \quad (2)$$

for the total field when the object is present in the imaging domain. The index r represents the receiving points. Φ is a calibration term of the unknown amplitude and phase difference between the experimental system and the numerical model.

The measured scattered field $\mathbf{E}^{\text{scatt}}_{\text{meas}}$ due to the object can be derived from the incident and total field measurements

$$\mathbf{E}^{\text{scatt}}_{\text{meas}}(r) = \mathbf{E}^{\text{tot}}_{\text{meas}}(r) - \mathbf{E}^{\text{inc}}_{\text{meas}}(r) \quad (3)$$

E. Numerical Tools

In order to simulate the data and then validate the performance of the robot data acquisition system, a 2-D scalar electromagnetic direct solver has been used. It consists of computing the complex values of the scattered field $\mathbf{E}^{scatt}(r)$ from the incident field $\mathbf{E}^{inc}(r)$, and a known object, characterized by its complex permittivity distribution $\varepsilon^*(r')$.

Herein, the transmitting antenna is supposed to generate an incident vertical TM polarized cylindrical wave, which illuminating an object, infinite and homogenous along the vertical axis. The object S, is surrounded by a homogeneous medium of complex permittivity ε_1^*. The dielectric contrast is then defined locally by the quantity $C(r')$ such that:

$$C(r') = k^2_{obj}(r') - k_1^2 , \quad (4)$$

with :

$$k^2_{obj}(r') = \omega^2 \mu_0 \varepsilon^*(r') \quad (5)$$

$$k_1^2 = \omega^2 \mu_0 \varepsilon_1^* \quad (6)$$

As mentioned above in equation (3), the total field $\mathbf{E}^{tot}(r)$ is considered as the superposition of the incident field $\mathbf{E}^{inc}(r)$ and the scattered field $\mathbf{E}^{scatt}(r)$. The scattered field results from the radiation of equivalent currents induced by the incident wave in the object. In such a way, the total electromagnetic field is given by an Electrical Field Integral Equation Formulation:

$$\mathbf{E}^{tot}(r) = \mathbf{E}^{inc}(r) + \iint_S \mathbf{G}(r,r')C(r')\mathbf{E}^{tot}(r')\,dr' \quad (7)$$

The Green function $\mathbf{G}$, which is the scattered field by a line source, is given by $\mathbf{G}(\mathrm{r},\mathrm{r}') = -j/4H_0^{(1)}(k_1|r-r'|)$. The index r represents the observation point, and r' the source point in the object domain S.

For its numerical computation the integral formulation is transformed to a discrete form, by applying a Method of Moments, with pulse basis functions and point matching:

$$\mathbf{E}^{\text{scatt}}(r_m) = \sum_{j=1}^{N} \mathbf{G}(r_m, r_j)C(r_j)\mathbf{E}^{\text{tot}}(r_j), \quad m = 1,2,\dots,M \quad (8)$$

where M represents the number of antennas positions and N the number of cells used for the object's discretization.

III. Experimental validation

First Experiments have been performed with a polycarbonate (PC) cylinder whose diameter is 110*mm*, (3 *mm* thick) and filled with sunflower oil (ε^* = 2.5+j0.1). The cylinder is placed at the center of a tank, filled by 10ºC water (ε_1^* = 83.2+j7.3) and whose dimensions are approximately 2*m* in diameter and 1.6*m* in high. In such a way, the non-reflection infinity assumption can be considered as valid. Moreover the complex permittivity of water which is supposed to be constant, is very sensitive to temperature variations, the use of such large amount of water helps to maintain the temperature constant during the experiments

The robot is configured to scan the object along a circular line of 55 points using the cylindrical surface mode with a radius of 225*mm* and a 5° angular step, sweeping 270° from 45° to 315°. The transmitter is located 114*mm* from the center at 0° in angular position. The signal to noise ratio (SNR) is measured to 45dB.

The comparison between the experimental and the simulated data at 1 GHz is shown in Fig. 6, for both amplitude and phase. Note that the calculated values obtained from the direct solver, are calibrated by applying a global amplitude and phase coefficient, which is equivalent to $\Phi \neq 1$ in equation (1) and (2). As one can see, very promising initial results are obtained: a well reproduced symmetry is observed, which means that the object is positioned with high accuracy, and a root mean square (RMS) error between the measured and simulated data less than 1.6dB in amplitude and 14º in phase is obtained. Note, that a good repeatability of the measurements, characterized by a RMS error less than 0.6dB in amplitude and 2.5º in phase, has been also observed.

Future work will be concerned with the characterization of the image reconstruction capabilities of the system. The complex permittivity distribution of the object will be computed with an inverse scattered solver based on a Newton-Kantorovitch iterative method [14], from a multi-incidence set of the Robot's data.

IV. Conclusion

In this paper a new flexible robot controlled microwave imaging system able to measure along cylindrical or half-spherical surfaces around the object has been presented. A first validation of the system has been performed for a sunflower oil filled tube, by measuring the scattered field along a circular arc around the object. Next, will be concerning with reconstruction of multi-view data from an inhomogeneous object, to test its ability in term of quantitative

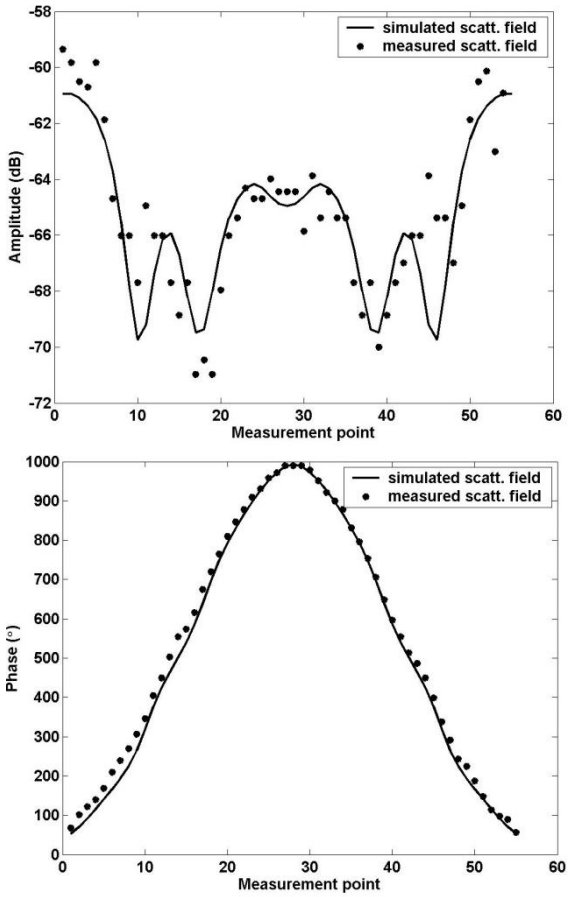

Fig. 6 Comparison between measured and simulated scattered field from a sunflower oil filled 110 mm diameter tube @ 1 GHz, amplitude (top), unwrapped phase (bottom).

imaging. Another challenge is to develop a realistic breast phantom, which needs a reliable and repeatable method for characterization of materials' dielectric properties.

Once validated, the flexibility of the system, in terms of geometry and positioning could offer new scenarios for future microwave imaging in both biomedical and industrial domains.

REFERENCES

[1] Paul M. Meaney, Margaret W. Fanning, Dun Li, Steven P. Poplack, and Keith D. Paulsen, "A Clinical Prototype for Active Microwave Imaging of the Breast," *IEEE Transactions on Microwave Theory and Techniques*, vol. 48, pp. 1841–1853, Nov. 2000.

[2] T. Gunnarsson, N. Joachimowicz, A. Diet, C. Conessa, D. Åberg, J.-C. Bolomey, "Quantitative Imaging Using a 2.45 GHz Planar Camera," *5th World Congress on Industrial Process Tomography*, Bergen Norway, Sept. 2007.

[3] L. E. Larsen and J. H. Jacobi, "Microwave Scattering Parameter Imaging on an Isolated Canine Kidney," *Medical Physics*, vol. 6, pp. 394-403, 1979.

[4] A. Joisel, J. Mallorqui, A. Broquetas, J. M. Geffrin, N. Joachimowicz, M. V. Iossera, L. Jofre and J. -C. Bolomey, "Microwave Imaging Techniques for Biomedical Applications," *Instrumentation and Measurement Technology Conference*, 1999.

[5] J. -C. Bolomey, L. Jofre and G. Peronnet "On the Possible Use of Microwave-Active Imaging for Remote Thermal Sensing," *IEEE Transactions on Microwave Theory and Techniques*, vol. 31, pp. 777-781, Sept. 1983.

[6] A. Franchois, A. Joisel, C. Pichot and J. -C. Bolomey, "Quantitative Microwave Imaging with a 2.45-GHz Planar Microwave Camera," *IEEE Transactions on Medical Imaging*, vol. 17, pp. 550-561, Aug. 1998.

[7] L. Jofre, M. S. Hawely, A. Broquetas, E. De Los Reyes, M. Ferrando and A. R. Elias-Fuste, "Medical Imaging with a Microwave Tomographic Scanner," *IEEE Transactions on Biomedical Engineering*, vol. 37, pp. 303-311, Mars 1990.

[8] A. Broquetas, J. Romeu, J. M. Rius, A. R. Elias-Fuste, A. Cardama and L. Jofre, "Cylindrical Geometry: A Further Step in Active Microwave Tomography," *IEEE Transactions on Microwave Theory and Techniques*, vol. 39, pp. 836-844, May 1991.

[9] Serguei Y. Semenov, Robert H. Svenson, Alexander E. Boulyshev, Alexander E. Souvorov, Vladimir Y. Borisov, Yuri Sizov, Andrey N. Starostin, Kathy R. Dezern, George P. Tatsis, and Vladimir Y. Baranov, "Microwave Tomography: Two Dimensional System for Biological Imaging," *IEEE Transactions on Biomedical Engineering*, vol. 43, pp. 869 – 877, Sept. 1996.

[10] Serguei Y. Semenov, Robert H. Svenson, Alexander E. Bulyshev, Alexander E. Souvorov, Alexei G. Nazarov, Yuri E. Sizov, Vitaly G. Posukh, Andrey Pavlovsky, Pavel N. Repin, Andrey N. Starostin, Boris A. Voinov, Michael Taran, George P. Tatsis, and Vladimir Y. Baranov," Three-Dimensional Microwave Tomography: Initial Experimental Imaging of Animals," *IEEE Transactions on Biomedical Engineering*, vol. 49, pp. 55 – 63, Jan. 2002.

[11] D. Li, P. M. Meaney and K. D. Paulsen, "Conformal Microwave Imaging for Breast Cancer Detection," *IEEE Transactions on Microwave Theory and Techniques*, vol. 51, pp. 1179-1186, April 2003.

[12] Paul M. Meaney, Keith D. Paulsen, Alexander Hartov, and Robert K. Crane, "An active microwave imaging system for reconstruction of 2-D electrical property distributions," *IEEE Transactions on Biomedical Engineering*, vol. 42, pp. 1017 – 1026, Oct. 1995.

[13] A.Stogryn, "Equations for calculating the dielectric constant of saline water", *IEEE Transactions on Microwave Theory and Techniques*, vol. 19, no. 8, pp.733-736, Aug. 1971.

[14] N. Joachimowicz, C. Pichot, and J. P. Hugonin, "Inverse Scattering: numerical method for electromagnetic imaging," *IEEE Transactions on Antennas and Propagation*, vol. 39, pp. 1742-1752, Dec. 1991.